Available online at www.sciencedirect.com
ScienceDirect
Trans. Nonferrous Met. Soc. China 25(2015) 1950−1960
Transactions of Nonferrous Metals Society of China
www.tnmsc.cn

Friction coefficient and microhardness of anodized aluminum alloys under different elaboration conditions

M. GUEZMIL[1], W. BENSALAH[1], A. KHALLADI[1], K. ELLEUCH[1], M. DEPETRIS-WERY[2], H.F. AYEDI[1]

1. Laboratoire de Génie des Matériaux et Environnement (LGME), ENIS, B.P. 1173-3038, University of Sfax, Tunisia;
2. IUT Mesures Physiques d'Orsay-University of Paris-Sud 11, Plateau du Moulon, 91400 Orsay, France

Received 23 July 2014; accepted 26 November 2014

Abstract: The effects of anodizing conditions (electrolyte, current density and temperature) on the friction coefficient and Vickers microhardness of anodic oxide layers formed on Al 5754 and Al 1050A substrates were investigated. The studied properties were examined using DELTALAB HVS−1000 Vickers microhardness tester and rotating pin on disc tribometer. It was established that the highest microhardness (>HV 400) and the lowest friction coefficient (<0.4) were obtained with the oxalic acid addition of 10 g/L at high current density of 3 A/dm^2 and low temperature of 5 °C. The presence of oxidized Mg through the anodic oxide layer formed on Al 5754 was examined using glow-discharge optical emission spectroscopy (GDOES). The MgO was found to act negatively on the mechanical property of the layer. Finally, the scanning electron microscopy (SEM), energy dispersive X-ray spectroscopy (EDS), and atomic force microscopy (AFM) were used to characterize the anodic layer before and after friction tests. It is found that the wear mechanism is related to many aspects of the initial morphology, chemical composition of the layer (C, S and Mg), porosity and internal stress.

Key words: aluminium alloy; anodization; friction coefficient; microhardness; dry sliding friction; surface characterization

1 Introduction

Wrought aluminum−magnesium alloys (5xxx) have been widely used in automotive, shipbuilding and engineering construction due to their light mass, good physical properties, corrosion resistance and low cost [1−4]. However, their use is limited because they are subject to deterioration due to low hardness and high friction. Their surface properties can be enhanced by applying suitable treatments such as anodizing [5−7]. Anodizing is a surface treatment process that can generate on aluminum and aluminum alloys, thick, hard and protective oxide layer [8−10].

It has been reported that the mechanical/tribological properties of anodic oxide layer depend on its porosity [11−13]. However, this porosity depends strongly on the anodizing operating conditions such as cell voltage and electrolyte composition [14−19]. Owing to this porosity, anodic oxide layers are very advantageous for tribological applications as they can be used as a reservoir for lubricants to form self-lubricating structures [20,21]. Many researchers have considered the tribological properties of their elaborated self-lubricating structure and demonstrated the enhancement in friction and wear performance to some levels [20,21].

HU et al [13] have conducted an enlargement treatment on their anodic structure and found an enhancement of friction coefficient due to the change of the pores forming from irregular to regular round. KIM et al [12] have studied friction and wear properties of anodic oxide layer in relation to contact load and pore diameter. They have observed a significant influence of pore size on the friction coefficient at relatively high loads and its decrease with the increase of load. VOJKUVKA et al [22] have demonstrated that the mechanical properties of anodic oxide layers not only depend on their porosities but also on the acid electrolyte used during the anodization. MEZLINI et al [8] have investigated the effect of sulphuric anodizing (SA) on the scratch damage of the 5xxx aluminum alloy used in transport application. They have concluded that SA treatment decreases abrasive wear resistance despite the increase of the anodized layer hardness. In our previous works [18,19], we have shown the benefic effect of oxalic acid adding to sulphuric acid bath on the wear

Corresponding author: W. BENSALAH; Tel: +216-74-274088; Fax: +216-74-275595; E-mail: walidbensalah@gmail.com
DOI: 10.1016/S1003-6326(15)63803-1

response of anodized aluminum using the methodology of experimental design.

However, we think that the friction behavior of anodic oxide layer need to be more investigated to be well utilized as self-lubricating structures.

The main focus of this work is to study the effect of anodizing conditions (temperature, current density and electrolyte composition) on the friction coefficient and Vickers microhardness of anodic oxide layers formed on Al 5754 and Al 1050A. Scanning electron microscopy (SEM), atomic force microscopy (AFM), glow-discharge optical emission spectroscopy (GDOES) and X-ray photoelectron spectroscopy (XPS) were used to characterize the elaborated oxide layers. On the basis of some of these characterization techniques, a wear mechanism was advanced.

2 Experimental

2.1 Materials and methods

1050A and 5754H111 aluminium alloys were used in this study. Chemical compositions of these materials are given in Table 1. Their Vickers microhardnesses were HV 28 and HV 67, respectively. Samples (100 mm × 25 mm × 3 mm) of both alloys were mechanically polished to P1000 grade paper followed by chemical polishing in a 15:85 (volume ratio) mixture of concentrated HNO_3 and H_3PO_4 at 85 °C for 2 min, etching in 1 mol/L NaOH solution at room temperature for 1 min and chemical pickling in 30% HNO_3 (volume fraction) solution at room temperature for 30 s. Water rinsing was used after each step. Afterwards, samples were anodized in vigorously stirred acid solution maintained within ±0.1 °C of the set temperature. Two acidic electrolytes were considered for anodizing: 1) 160 g/L sulphuric acid bath and 2) mixture of 10 g/L oxalic acid and 160 g/L sulphuric acid. Whatever the anodizing conditions are, the anodizing duration was chosen so that to obtain oxide layer thicknesses of 30 μm measured using ELCOMETER 355 top thickness gauge equipped with eddy current probe. It is to mention that the used cathodes were also aluminum sheets. Sulphuric and oxalic acids were analytical grade chemicals.

2.2 Testing methods

2.2.1 Microhardness measurement

Vickers microhardness of the anodic film was carried out using a Vickers microhardness tester DELTALAB HVS−1000 (200 g load for 15 s as dwell time). Results are the average of 10 measurements for every specimen.

2.2.2 Friction test

Friction tests were carried out under dry conditions using a pin-on-disc tribometer. Anodized samples with dimensions of 20 mm × 20 mm × 3 mm were brought into contact with 100C6 steel ball with a diameter of 6 mm. All tests were performed at the same sliding speed of 100 r/min (0.052 m/s). The applied normal load was 1 N.

Friction tests were performed in ambient air (25−27 °C) at relative humidity (RH) of 35%−45%. During tests, the variation of the friction coefficient versus time was recorded.

2.2.3 Surface morphology

The morphology of the oxide layer was studied from the top side of the layer using a scanning electron microscope SEM-FEG (Jeol JSM−6400F). AFM characterization, using model digital instrument-nanoscope probe II (contact mode), was realized to examine the roughness of the anodized surfaces. Surface topography was recorded over a scanned area of 5 μm × 5 μm.

The wear tracks were studied using a LEICA optical microscope and a TESCAN VEGA II scanning electron microscope (SEM) coupled with an energy-dispersive X-ray spectroscopy (EDS) for chemical analysis.

2.2.4 Glow-discharge optical emission spectroscopy (GDOES)

Chemical species in the anodic layers were determined by depth profiling using a Jobin Yvon GD profiler instrument equipped with an anode of 4 mm in diameter and working at a pressure of 800 Pa and a power of 600 W in an argon atmosphere. The relevant wave-lengths were as follows: Al, 396.15 nm; O, 130.22 nm; S, 181.73 nm and C, 156.14 nm. The sputtered layer was 6 μm in thickness.

2.2.5 X-ray photoelectron spectroscopy (XPS) analysis

XPS measurements were performed with a PHI Quantera SXM electron spectrometer operated at a power of 50 W. Abrasions were carried out using Ar^+ ion beam. The pressure in the chamber was maintained below 1.33×10^{-7} Pa during analysis. In order to regularize the heterogeneity of the coatings, survey spectra were taken from at least three measurement areas

Table 1 Chemical compositions of Al 1050A and Al 5754 aluminum substrates (mass fraction, %)

Alloy	Si	Mn	Cu	Ti	Zn	Fe	Pb	Mg	Al
Al 1050A	0.11	<0.005	<0.005	0.014	0.009	0.37	0.006	<0.005	Bal.
Alloy	Si	Fe	Cu	Mn	Mg	Cr	Zn	Ti	Al
Al 5754	<0.40	<0.40	<0.10	<0.50	2.6−3.6	<0.30	<0.20	<0.15	Bal.

in each oxide layer. All spectra were collected at an electron take-off angle of 45° from coating areas of 200 μm. The analysis depth was inferior to 10 nm. The relative amounts of all the bound carbons were found from high-resolution C 1s spectra (peak at 285 eV) via symmetric Gaussians.

3 Results and discussion

3.1 Vickers microhardness of anodic oxide layer

Figure 1(a) illustrates the influence of the anodizing temperature on the Vickers microhardness of the anodic oxide layer elaborated under galvanostatic conditions (2 A/dm^2). As can be seen, the microhardness decreases with increasing anodizing temperature whatever the electrolyte composition and the substrate are. Indeed, it is well established that dissolution at the interface oxide/electrolyte is more important at high temperature [5]. These results are in agreement with those of AERTS et al [11] who found that the oxide formed at low temperatures has a dense structure with small pores separated by thick walls, while the increase of electrolyte temperature leads to more open pores and low hardness. From them, MOUTARLIER et al [17] showed that the increase of temperature favors the layer formation, i.e., the thickness of anodic layer is large, but magnifies the surface porosity.

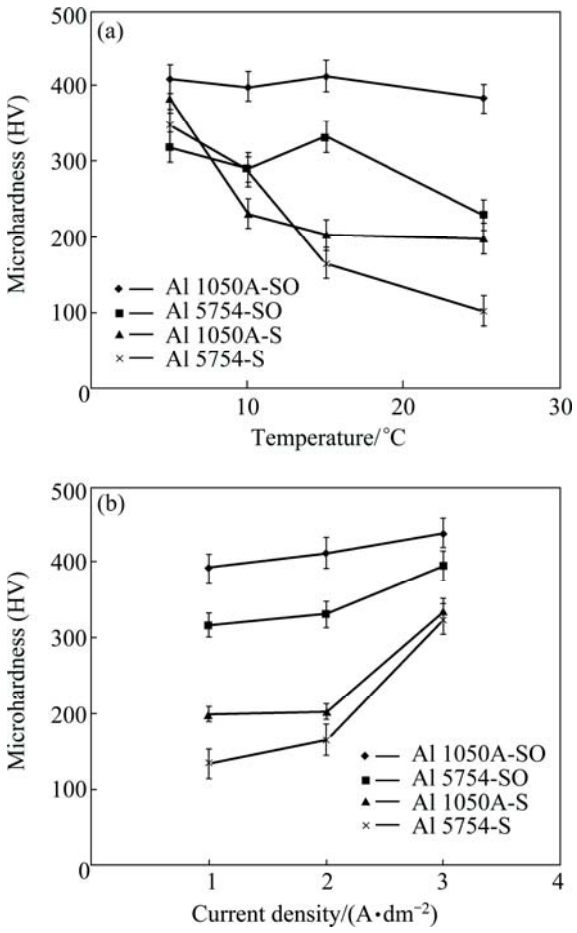

Fig. 1 Vickers microhardness of anodic oxide layers formed on Al 1050A and Al 5754 substrates against (Acid baths: sulphuric (S), sulphuric−oxalic (SO)): (a) Anodizing temperature; (b) Current density

The Vickers microhardness values of anodic oxide layers elaborated in sulphuric−oxalic acid mixture are higher than those elaborated in sulphuric acid bath (Figure 1(a)). These results are consistent with those of MOUTARLIER et al [17] who demonstrated that oxalic acid addition has a benefic effect on the film formation. They have also shown that the increase of oxalic acid concentration in the anodizing bath decreases the surface porosity and anodic layers are more compact [17]. This finding may be attributed to the decrease of aggressiveness of the acid mixture by the addition of oxalic acid [17,19]. The adding of weak acid (oxalic acid) to sulphuric acid (strong acid) enhances the oxide layer growth, reduces the dissolution reactions at the interface oxide/electrolyte as well as from the pore walls and performs compacter layers.

Figure 1(b) shows the influence of the current density on the Vickers microhardness of the anodic oxide layer elaborated at 15 °C. The microhardness increases with increasing current density whatever the bath and the substrate are. These results are similar to those found by APACHITEI et al [14] when they studied the anodizing of AlSi(Cu) substrate. They have found an increase of oxide layer microhardness with the increase of current density in the range of 0−3 A/dm^2. Increasing current density leads to an increase in layer thickness and electrical field strength. These effects can generate larger gradients of composition along the deeper pore walls by adsorption of sulfate anions [14]. In the studied domain (1−3 A/dm^2), the Vickers microhardness values of anodic oxide layers elaborated in sulphuric−oxalic acid mixture are higher than those elaborated in sulphuric bath (Figs. 1(a) and (b)).

Furthermore, the alloying element seems to influence the microhardness of the layer. The microhardness values obtained for anodic oxide layers elaborated on Al 5754 are smaller than those obtained on Al 1050A. The observed difference can be explained by the presence of magnesium oxide in the layer. As far as we are concerned, further explanation will be given later.

3.2 Friction coefficient

In this section, friction behaviour of the aluminium substrates was investigated. The variation of the friction coefficient of the studied substrates vs time is shown in Fig. 2. As can be seen, this plot reveals three regions linked to three regimes: friction first increases, then decreases and finally achieves a steady state value for the

rest of the sliding distance. The changes of the friction coefficient values can be coupled with the evolution of the wear morphology and the degree of oxidation. These results are in accordance with those of KIM et al [23]. In fact, they demonstrated the significant role of oxygen on the wear morphology changes. Besides, YEROKHIN et al [24] related this finding to the transition from the wear mechanism of the couple steel/aluminium (ductile) to that of steel/oxide film (brittle) formed by oxidation which decreases the friction coefficient. The little difference in the friction coefficient between the two substrates seems to be attributed to the difference in their hardness and/or chemical composition.

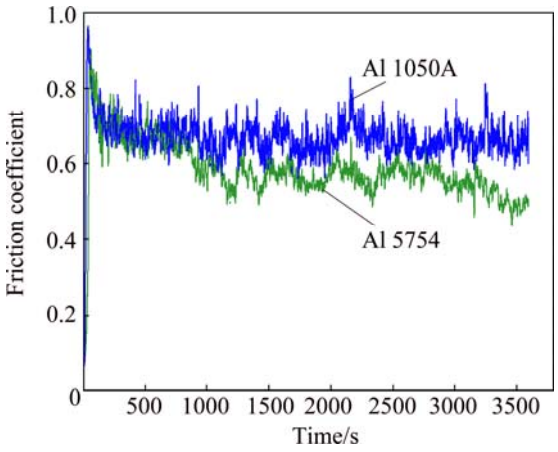

Fig. 2 Friction coefficients of Al 1050A and Al 5754 substrates against sliding time

Figure 3(a) depicts the friction coefficient evolution vs sliding time of anodic oxide layers formed in sulphuric acid bath at different temperatures. The friction coefficient increases with the increase of temperature for both anodized substrates and is lower for Al 1050A whatever the temperature is. It is important to mention that a better friction property is reached with layers formed at low temperatures. Figure 3(b) illustrates the friction coefficient of anodic oxide layers elaborated in sulphuric−oxalic acid bath against the sliding time at 5 and 25 °C. The same conclusions can be emitted in term of dependence of the friction coefficient with anodizing temperature. With regards to the obtained results, the anodic oxide layers formed in sulphuric−oxalic acid bath present the best friction coefficient whatever the substrate is.

At this stage, it is possible to relate, to some level, the friction coefficient of the anodized layers to their microhardnesses as it varies similarly as a function of the elaboration conditions.

The influence of the anodic current density on the friction coefficient evolution for the oxide layers elaborated in the studied bathes is shown in Fig. 4. The friction coefficient decreases with the increase of the

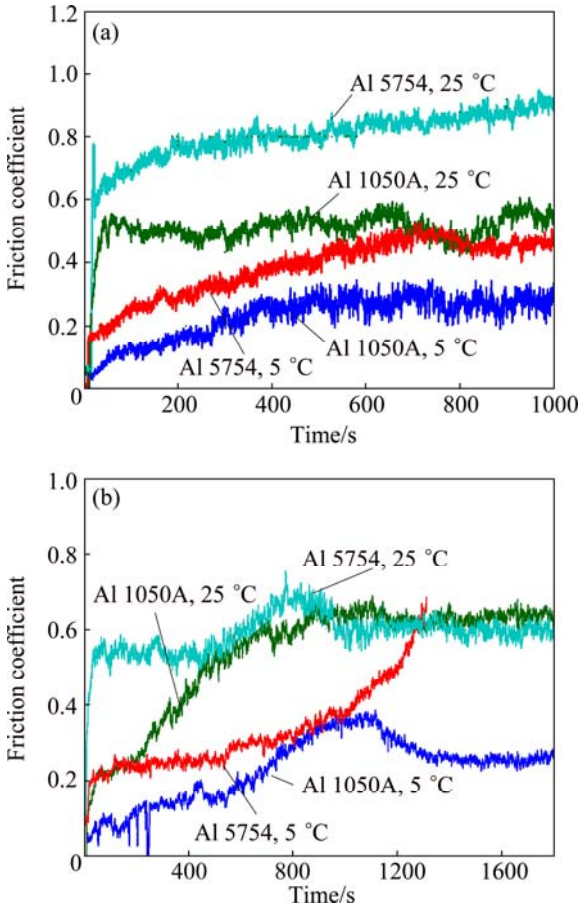

Fig. 3 Friction coefficients of anodic oxide layers formed on Al 1050A and Al 5754 substrates in sulphuric acid bath (a) and sulphuric−oxalic acid bath (b) as function of sliding time and anodizing temperature

anodic current density. Moreover, the current density also affects the shape of the curve; at low current density (1 A/dm^2), the friction coefficient reaches rapidly the quasi-stationary levels (0.5−0.7) whilst, at 3 A/dm^2, the same values are obtained when the time is extended to 500 s (Fig. 4). As previously concluded, the friction coefficient values measured on anodic oxide layers formed on Al 1050A are higher than those obtained with layers formed on Al 5754 whatever the current density is. The analysis of Fig. 4 shows that anodic oxide layers formed at high current density in sulphuric−oxalic acid bath present the best friction coefficient for both anodized substrates.

As remarked previously, the friction coefficient and the Vickers microhardness vary in the same way when considering the current density.

In view of the friction coefficient responses (Figs. 3 and 4), it is to remark a difference in tendencies at the beginning (slope) compared with the aluminum substrates and anodized layers. This difference may be related to the difference of microhardness. Since the microhardness of the aluminum is much lower than that

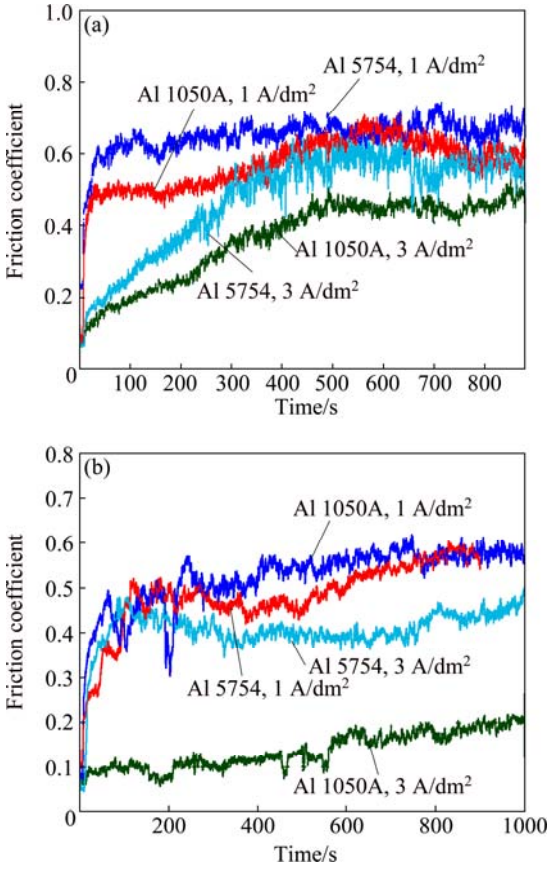

Fig. 4 Friction coefficients of anodic oxide layers formed on Al 1050A and Al 5754 substrates in sulphuric acid bath (a) and sulphuric−oxalic acid bath (b) as function of sliding time and current density

of the anodic layer. LEE et al [25] ascribed this finding to the existence of more microscopic junctions between the asperities of aluminum substrates and the steel ball. The change tendency in the friction coefficient may also be attributed to the formation of a tribolayer [25].

In order to study the effect of the oxide porosity on the friction coefficient, an enlargement treatment was conducted by immersion of anodized samples in 5% (mass fraction) of phosphoric acid and at 30 °C under different durations [13].

Figure 5 shows the variation of the friction coefficient when the pores of anodic layers are enlarged after 20 and 40 min of immersion compared with untreated sample. The quasi-stationary value of the friction coefficient obtained after 20 min of immersion is smaller than that of untreated specimen. This finding can be related to the changes of the pores form from irregular to regular round, which is in accordance with the results of HU et al [13]. They have proved that surface with regular round pores possesses better tribological properties [13]. For 40 min of pore-enlargement, the friction coefficient is higher. As can be concluded, prolonged pore-enlargement treatment makes the cell

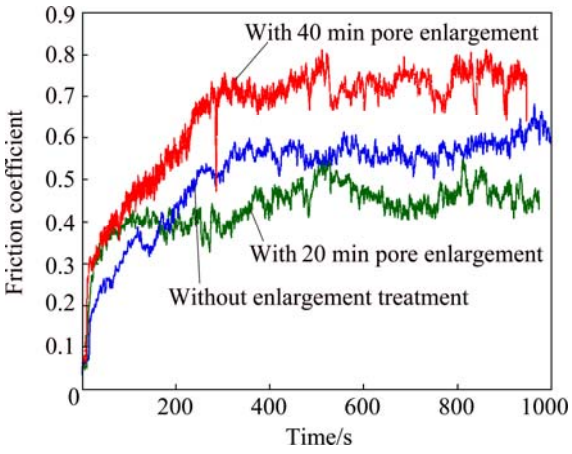

Fig. 5 Friction coefficients of anodic oxide layers formed on Al 5754 in sulphuric acid bath with and without pore enlargement treatment

wall weak, so the ability of the whole anodic structure to sustain normal pressure is reduced.

3.3 Effect of morphology and chemical composition on wear mechanism of anodic layer

After the sliding tests, wear tracks were analyzed by SEM (Fig. 6). Figures 6(a)−(d) demonstrated the presence of smooth tribolayers formed by the combined influence of tribochemical reaction as well as material transfer on the contact surface. The observed smoothness suggested the generation of severe plastic deformation of compressed debris. The optical microscopy of the worn surface of the steel ball (Fig. 6(e)) shows, equally, degradations. In fact, the EDS spectra shown in Fig. 7 reveal that the wear tracks are composed of Fe and Mo, originated from the components of the ball, and Al and O, the main chemical elements of the coatings. This explains that active tribochemical reaction and material transfer occurred between the mating materials.

It is noted that the energy involved in contact with the work of friction force is very important. This dissipates in the environment and in each of the two counterparts, causing them to be heated. These thermal phenomena play a decisive role in various changes that will occur during sliding. Under the simultaneous action of local overstressing and overheating, the steel ball and the anodic oxide layer will be subjected to geometric and chemical modifications.

One of these manifestations is illustrated in Figs. 6(a)−(d). SEM image analysis reveals cracks besides wear tracks (Figs. 6(a)−(d)). As can be seen, linear cracks are created along the sliding direction following the frontward movement of the steel ball on the surface of the oxide layers. All cracks have identical angle with regard to the sliding direction. This means that, during sliding, the cracks are together formed on

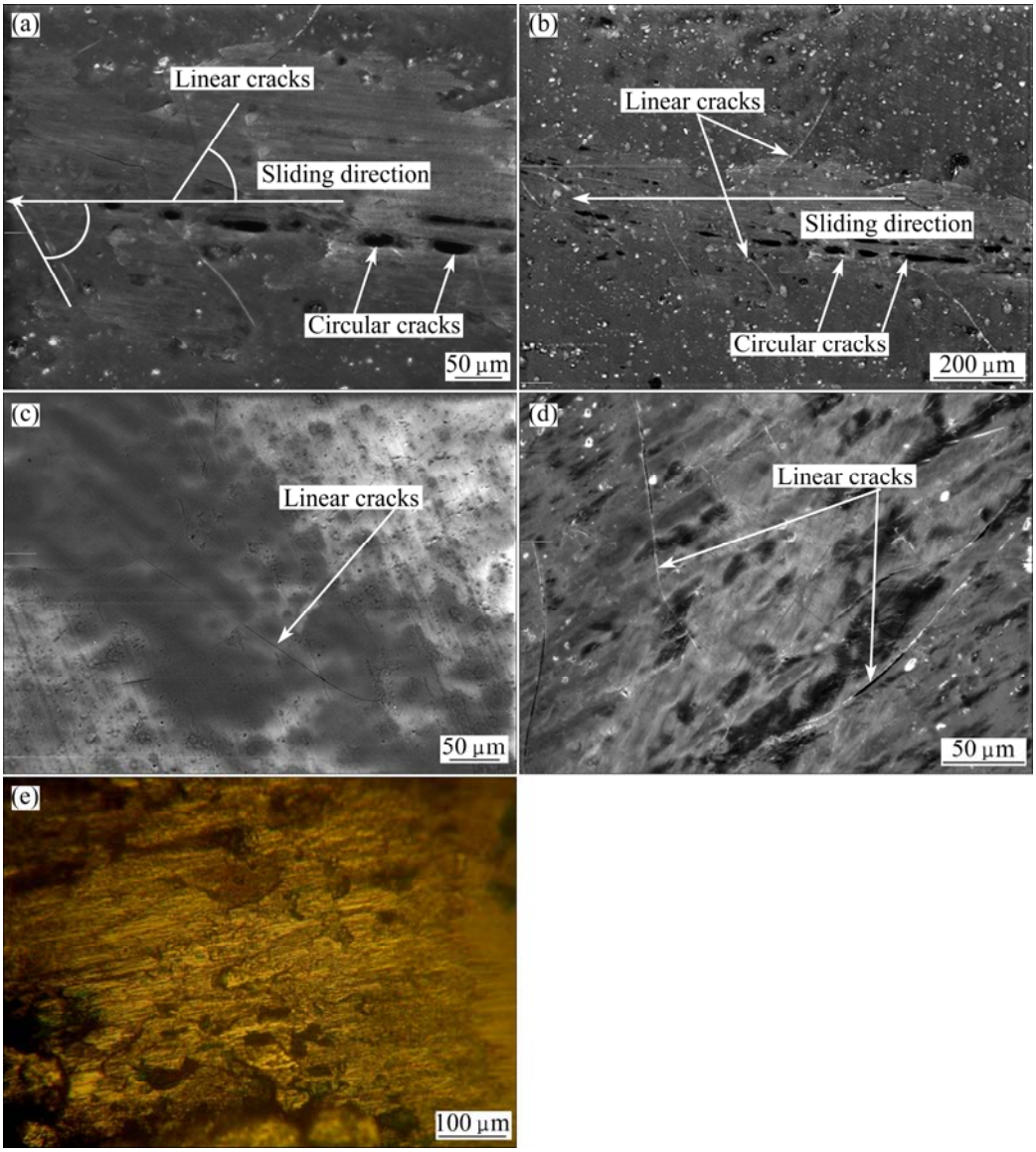

Fig. 6 SEM images of worn surfaces of anodic oxide layers formed in sulphuric acid bath (a, b) and sulphuric−oxalic acid bath (c, d): (a, d) 5 °C, 2 A/dm^2; (b, c) 25 °C, 2 A/dm^2; (e) OM of worn surface of steel ball

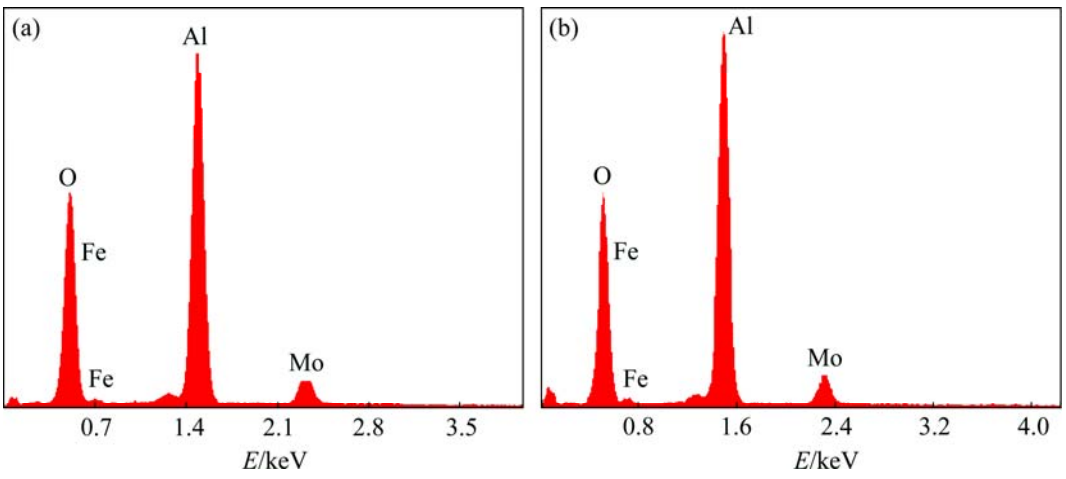

Fig. 7 EDS analysis of wear debris and worn surfaces of anodic oxide layers formed on Al 5754 in sulphuric acid bath: (a) 5 °C, 2 A/dm^2; (b) 25 °C, 2 A/dm^2

both sliding sides along the wear scars. The obtained result is in accordance with that of VOJKUVKA et al [22] when the anodized layer is characterized by scratch test. In fact, they demonstrated that the pore cells were deformed on the indent sides, and collapsed following a direction parallel to the crack [22]. The collapsing and shape deformation of pores were equally observed by PAPKA and KYRIAKIDES [26] on large-scale porous metals and polymers with honeycomb structure under shear. Shear forces induced by the steel ball during the loading cycle seem to be the first cause of the observed fractures.

In addition to the linear cracks present on the wear tracks sides, circular cracks are also formed through the wear scars (Fig. 6). Those circular cracks may be induced by the high stress under the steel ball. It is possible that these circular cracks are the result of the collapse of the oxide layer. In fact, they are formed behind the steel ball after the release of the compressed pore cells [22].

With regard to the whole conducted SEM images (not shown here), the crack formation is variable. In fact, anodic oxide layers are rather brittle and stiff, but some others are more able to deform under sliding tests without significant breaking up. This behavior can be ascribed to the elaboration conditions (temperature, current density and acid solution).

SEM−FEG and AFM were used for surface characterization before friction tests. SEM images give a surface view over a relatively large area and AFM analyzes the chosen surface with 3D images. The limited scan area of AFM image may result in surface images that are not representative of the entire surface, but can give good ideas of surface details.

The SEM examination of the anodized layers shows characteristic rough domes, cavities and cracks probably due to the internal stress (Fig. 8).

The topography of anodic oxide layers observed by AFM presents, equally, domes and cavities (Fig. 9). This morphology demonstrates the effect of elaboration conditions on the surface state of the oxide and consequently, results in non-uniform stress distribution and local concentration of the stress under the steel ball during sliding tests.

In fact, AERTS et al [11] demonstrated that the evolution of the wear resistance of anodized layers as a function of the electrolyte temperature approximately matched the evolution of anodic layer porosity. They suggest that the increase of bath temperature increases the aggressiveness of the acid electrolyte, especially in the near surface oxide region which will be exposed to a chemical dissolution. The latter can also produce open porosities, cavities and some local perturbation of the outer region of the layer. From geometrical point of view,

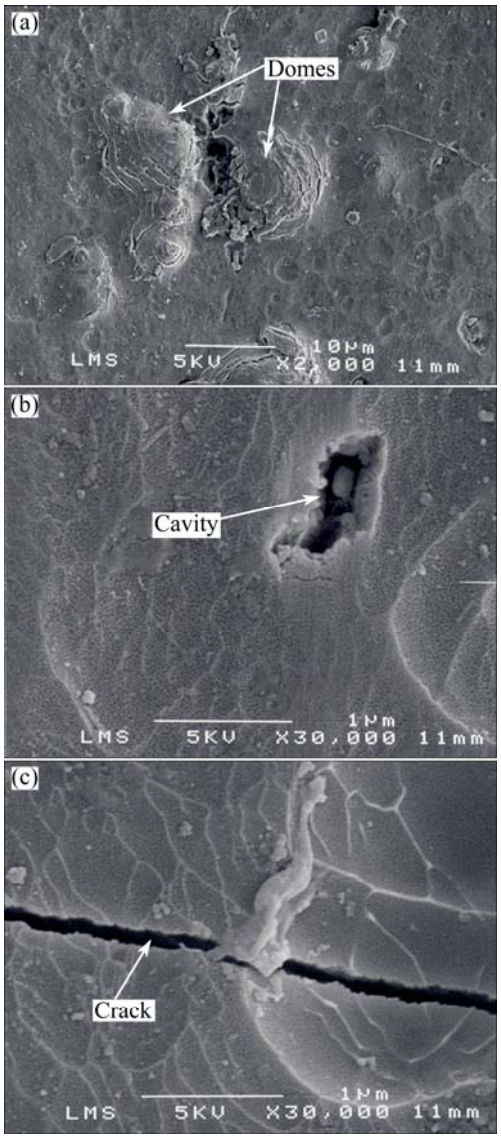

Fig. 8 SEM top view images of anodic layers elaborated in sulphuric−oxalic acid bath: (a, b) 25 °C, 2 A/dm^2; (c) 5 °C, 2 A/dm^2

the porosity of the layer can affect its friction behavior. In fact, the movement of the steel ball will not be the same on large and small pore diameters, which was confirmed previously by the results of the enlargement treatment. The obtained morphology seems to play a key role in the friction behaviour of the anodic layer.

The morphology of the oxide layer can conduct to other chemical phenomena. It is known that the anodic oxide layer contains voids due to oxygen evolution [27,28]. These voids are privileged seats for chemisorption of OH— groups and adsorption of water from the anodizing electrolyte since the hydroxide film formation will be favored by a combination of contact pressure, local temperature, and tribochemical reactions between air and humid oxide layers [29]. LEE et al [25] demonstrated that the pressure exerted to the surface

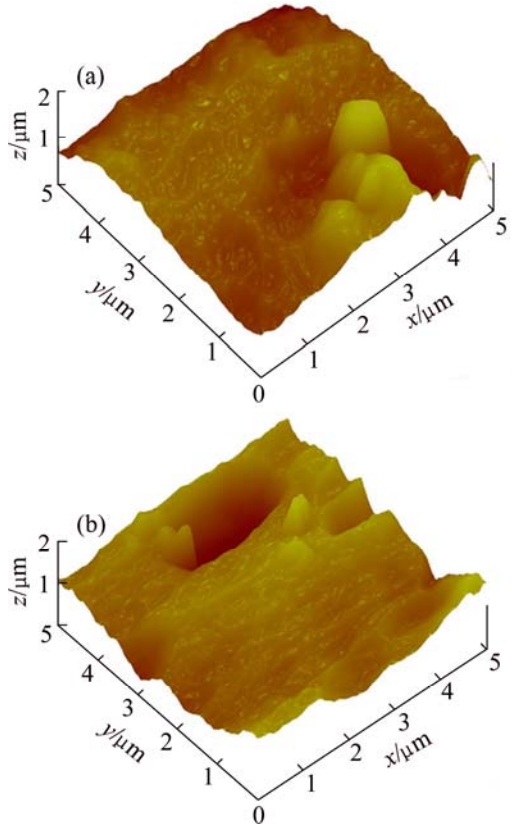

Fig. 9 AFM images of anodic layers elaborated in sulphuric−oxalic acid bath: (a) 5 °C, 2 A/dm^2; (b) 25 °C, 2 A/dm^2

of the oxide layer induces the deformation of the pores, and infiltrated water is released to form hydroxide on the surface. These hydroxides significantly change the wear response of anodic oxide layers [29].

Turning to the effect of substrate, the decrease of friction coefficient of layers formed on Al 5754 seems to be related to the alloying elements. In fact, anodic oxide layer formed on Al 5754 contains Al_2O_3 and magnesium oxide (MgO) [30]. ZHOU et al [30] demonstrated that Mg^{2+} ions are ejected more rapidly to the oxide/electrolyte interface, which permits a uniform distribution through the oxide layer. On the other hand, it was established that the microhardness of MgO is lower than that of Al_2O_3 [3].

In order to examine the presence of Mg through the anodic oxide layer formed on Al 5754, chemical analysis was conducted using GDOES (Fig. 10). Figures 10(a) and (b) show the presence of Mg, Al, O and S species. The presence of Mg, Al and O can be attributed to MgO and Al_2O_3 formation [3]. Mg element seems to be uniform throughout the layer. The existence of sulphur can be explained by the inward migration of sulphate anions through the pores of the coating [31]. The sulphate anions are located at the inner part of pores as shown by the peak of both S profiles (Figs. 10(a) and (b)).

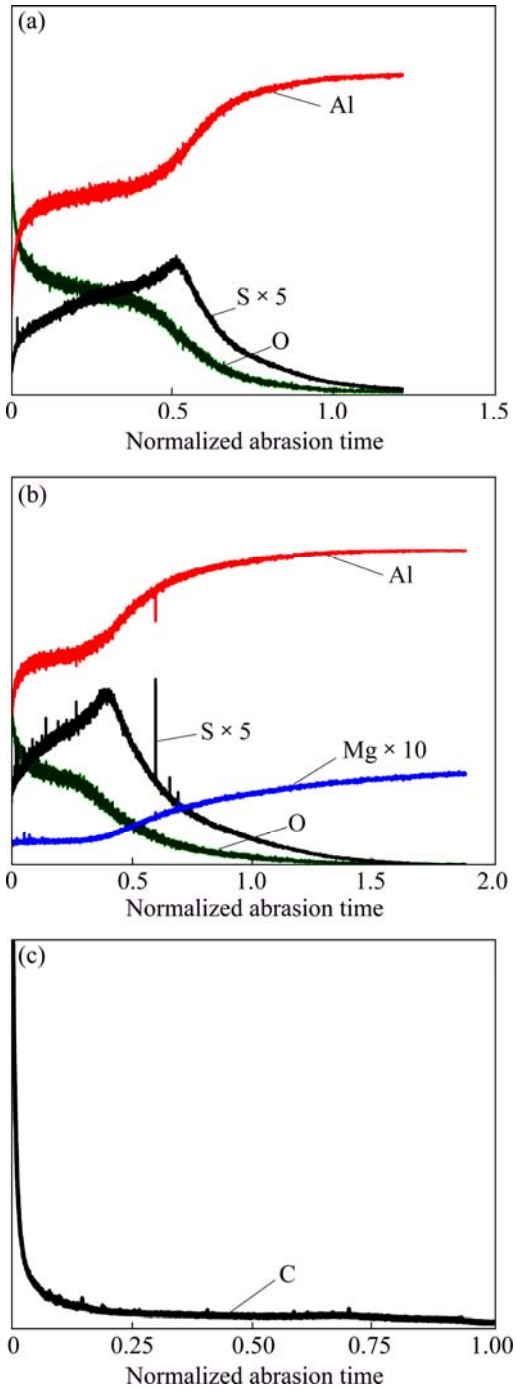

Fig. 10 GDOES of anodic oxide layers: (a) Al 1050A; (b) Al 5754, sulphuric bath at 25 °C, 2 A/dm^2; (c) Carbon profile of anodized Al 5754 in sulphuric−oxalic acid bath at 25 °C and 2 A/dm^2

It is well known that the anodic oxide layer is duplex and formed of pure and anion-contaminated alumina [31]. The ratio of the contaminated to pure alumina depends on the acid bath used for anodizing [31,32]. SHIMIZU et al [32] show that the incorporated carbon was in the form of $(COO^-)_2$ anions.

Accordingly, it is possible to relate, to some level,

the friction behavior of anodic oxide layers to the anion-contamination. However, it is possible that carbon species incorporated from sulphuric−oxalic acid bath into the oxide during anodization grants more compactness and/or lubricity to the anodized layer formed than that produced in sulphuric acid bath.

The examination of GDOES carried out on anodic oxide layer elaborated in sulphuric−oxalic acid bath shows that C profiles present always an intense peak on the outer surface (Fig. 10(c)). In order to deeply investigate the nature of carbon on the outer surface of the layer, XPS technique was used. XPS spectra acquired from the analyzed anodic oxide layer are shown in Fig. 11. Figure 11 shows mainly the presence of O, C and Al on the surface of the coating. Their chemical compositions in mass fraction are 36.6% C, 42.7% O and 12.8% Al.

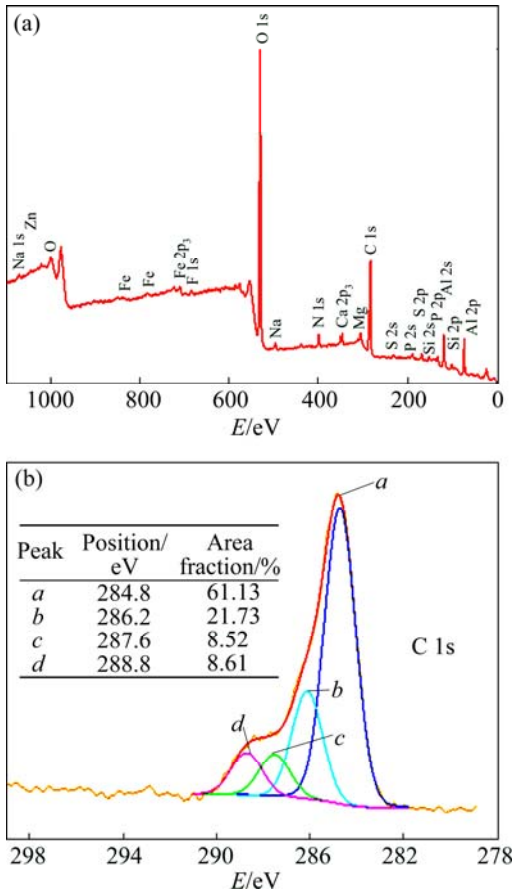

Fig. 11 X-ray survey spectrum of all elements from selected areas in anodic oxide layer (a), high resolution C 1 s spectra from same selected area taken from surface of coating (b) (Anodized Al 1050 in sulphuric−oxalic acid bath at 25 °C and 2 A/dm^2)

Figure 11(b) shows high resolution C 1s spectra from the same selected area taken from the surface of the coating. The examination of this figure reveals four peaks: 1) peak at 284.8 eV associated with C—C/C—H bonds with 60% of content; 2) peak at 286.2 eV related to C—O and/or C—N bonds with 22% of content; 3) peak at 287.6 eV coupled with O—C—O and/or C═O bonds with 9% of content and 4) peak at 288.8 eV associated with O—C═O bond with 9% of content. It is to mention that C—C/C—H situated on the extreme surface seems to be originated from contamination [33].

4 Conclusions

1) Vickers microhardness values of Al 1050A and Al 5754 increase with the increase of current density and decreases with temperature whatever the bath and the anodized substrate are.

2) Vickers microhardness values of anodic oxide layers elaborated on Al 1050A are higher than those obtained with Al 5754. Vickers microhardness values of anodic oxide layers elaborated in sulphuric−oxalic acid bath are higher than those elaborated in sulphuric bath.

3) The friction coefficient increases with the increase of temperature and decreases with the increase of current density. The friction coefficients measured on anodic oxide layers formed on Al 1050A are higher than those obtained with anodic layers formed on Al 5754 whatever the temperature and current density are. The alloying elements seem to act negatively on the layer performance. Anodic oxide layers formed in sulphuric−oxalic acid bath present the best friction coefficient whatever the condition is.

4) On the basis of the used characterizing techniques (SEM, AFM, EDS GDOES and XPS), it was found that the friction behaviour of anodic oxide layer depends on the elaboration conditions.

5) The wear mechanism is complex and related to many factors of the initial morphology, chemical compositions of the layer (C, S and Mg), porosity, internal stress, infiltrated water, contact temperature, local stress and environment.

Acknowledgements

This work was supported by the Ministry of Higher Education and Scientific Research, Tunisia.

References

[1] BAUMEISTER J, BANHART J, WEBER M. Aluminium foams for transport industry [J]. Materials and Design, 1997, 18: 217−220.

[2] BANHART J. Manufacture, characterization and application of cellular metals and metal foams [J]. Progress in Materials Science, 2001, 46: 559−632.

[3] ALISCH G, NICKEL D, LAMPKE T. Simultaneous plasma-electrolytic anodic oxidation (PAO) of Al−Mg compounds [J].

Surface & Coatings Technology, 2011, 206: 1085−1090.

[4] ZHOU X, THOMPSON G E, SKELDON P, WOOD G C, SHIMIZU K, HABAZAKI H. Film formation and detachment during anodizing of Al−Mg alloys [J]. Corrosion Science, 1999, 41: 1599−1613.

[5] YOUNG L. Anodic oxide films [M]. London: Academic Press, 1961.

[6] WERNICK S, PINNER R, SHEASBY P. The surface treatment of aluminum and its alloys [M]. 5th ed. London: Finishing Publication Ltd., 1987.

[7] SHEASBY P G, PINNER B. The surface treatment and finishing of aluminum and its alloys [M]. 6th ed. London: Finishing Publications Ltd., 2001.

[8] MEZLINI S, ELLEUCH K, KAPSA Ph. The effect of sulphuric anodization of aluminum alloys on cotact problems [J]. Surface and Coating Technology, 2007, 201: 7855−7864.

[9] BENSALAH W, FEKI M, WERY M, AYEDI H F. Thick and dense anodic oxide layers formed on aluminum in sulphuric acid bath [J]. Journal of Material Science and Technology, 2010, 26: 113−118.

[10] MAEJIMA M, SARUWATARI K, ISAWA K. Abrasion resistance of anodized coatings on aluminium alloys tested with an abrasive metal wheel wear tester [J]. Metal Finishing, 1998, 10: 36−41.

[11] AERTS T, DIMOGERONTAKIS T H, de GRAEVE I, FRANSAER J, TERRYN H. Influence of the anodizing temperature on the porosity and the mechanical properties of the porous anodic oxide film [J]. Surface & Coatings Technology, 2007, 201: 7310−7317.

[12] KIM H S, KIM D H, LEE W, CHO S J, HAHN J H, AHN H S. Tribological properties of nanoporous anodic aluminum oxide film [J]. Surface & Coatings Technology, 2010, 205: 1431−1437.

[13] HU Ning-ning, GE Shi-rong, FANG Liang. Tribological properties of nano-porous anodic aluminium oxide template [J]. Journal of Central South University of Technology, 2011, 18: 1004−1008.

[14] APACHITEI L E F, DUSZCZYK J, KATGERMAN L. Vickers microhardness of AlSi(Cu) anodic oxide layers formed in H_2SO_4 at low temperature [J]. Surface & Coatings Technology, 2003, 165: 309−315.

[15] JIA Y, ZHOU H, LUO P, LUO S, CHEN J, KUANG Y. Preparation and characteristics of well-aligned macroporous films on aluminum by high voltage anodization in mixed acid [J]. Surface & Coatings Technology, 2006, 201: 513−518.

[16] SULKA G D, PARKOLA K G. Anodizing potential influence on well-ordered nanostructures formed by anodisation of aluminium in suphuric acid [J]. Thin Solid Films, 2006, 515: 338−345.

[17] MOUTARLIER V, GIGANDET M P, PAGETTI J, NORMAND B. Influence of oxalic acid addition to chromic acid on the anodising of Al 2024 alloy [J]. Surface and Coatings Technology, 2004, 182: 117−123.

[18] BENSALAH W, ELLEUCH K, FEKI M, WERY M, AYEDI H F. Optimization of anodic layer properties on aluminum in mixed oxalic/sulphuric acid bath using statistical experimental methods [J]. Surface & Coatings Technology, 2007, 201: 7855−7864.

[19] BENSALAH W, ELLEUCH K, DE-PETRIS WERY M, AYEDI H F. Comparative study of mechanical and tribological properties of alumina coatings formed on aluminum in various conditions [J]. Materials and Design, 2009, 30: 3731−3737.

[20] MAEJIMA M, SARUWATARIA U K, TAKAYA M. Friction behaviour of anodic oxide film on aluminum impregnated with molybdenum sulfide compounds [J]. Surface & Coating Technology, 2000, 132: 105−110.

[21] TAKAYA M, HASHIMOTO K, TODA Y, MAEJIMA M. Novel tribological properties of anodic oxide coating of aluminum impregnated with iodine compound [J]. Surface & Coating Technology, 2003, 169: 160−162.

[22] VOJKUVKA L, SANTOS A, PALLARÈS J, FERRÉ-BORRULL J, MARSAL L F, CELIS J P. On the mechanical properties of nanoporous anodized alumina by nanoindentation and sliding tests [J]. Surface & Coatings Technology, 2012, 206: 2115−2124.

[23] KIM H J, EMGE A, KARTHIKEYAN S, RIGNEY D A. Effects of triboxidation on sliding behavior of aluminium [J]. Wear, 2005, 259: 501−505.

[24] YEROKHIN A L, NIE X, LEYLAND A, MATTHEWS A, DOWEY S J. Plasma electrolysis for surface engineering [J]. Surface & Coating Technology, 1999, 122: 73−93.

[25] LEE G S, CHOI J H, CHOI Y C, BU S D, LEE Y Z. Tribological effects of pores on an anodized Al alloy surface as lubricant reservoir [J]. Current Applied Physics, 2011, 11(S): s182−s186.

[26] PAPKA S D, KYRIAKIDES S. Experiments and full-scale numerical simulations of in-plane crushing of honeycomb [J]. Acta Materialia, 1998, 46: 2765−2776.

[27] ONO S, ICHINOSE H, MASUKO N. Defects in porous anodic films formed on high purity aluminum [J]. Journal of Electrochemical Society, 1991, 138: 3705−3710.

[28] ONO S, ICHINOSE H, MASUKO N. Lattice images of crystalline anodic alumina formed on a ridged aluminum substrate [J]. Journal of Electrochemical Society, 1992, 139: L80−L81.

[29] PALIBRODA E, MARGINEAN P. Considerations on the adsorbed water concentration of sulfuric porous aluminium oxide [J]. Thin Solid Films, 1994, 240: 73−75.

[30] ZHOU X, THOMPSON G E, SKELDON P, WOOD G C, SHIMIZU K, HABAZAKI H. Film formation and detachment during anodizing of Al−Mg alloys [J]. Corrosion Science, 1999, 41: 1599−1613.

[31] SHIMIZU K, HABAZAKI H, SKELDON P, THOMPSON G E, WOOD G C. Migration of sulphate ions in anodic alumina [J]. Electrochimica Acta, 2000, 45: 1805−1809.

[32] SHIMIZU K, HABAZAKI H, SKELDON P, THOMPSON G E, WOOD G C. Migration of oxalate ions in anodic alumina [J]. Electrochimica Acta, 2001, 46: 4379−4382.

[33] HOUMARD M, BERTHOME G, BOULANGE L, JOUD J C. Surface physico-chemistry study of an austenitic stainless steel: Effect of simple cold rolling treatment on surface contamination [J]. Corrosion Science, 2007, 49: 2602−2611.

不同加工条件下阳极化铝合金的摩擦因数和显微硬度

M. GUEZMIL[1], W. BENSALAH[1], A. KHALLADI[1], K. ELLEUCH[1], M. DEPETRIS-WERY[2], H.F. AYEDI[1]

1. Laboratoire de Génie des Matériaux et Environnement (LGME),
ENIS, B.P. 1173-3038, University of Sfax, Tunisia;
2. IUT Mesures Physiques d'Orsay-University of Paris-Sud 11, Plateau du Moulon, 91400 Orsay, France

摘　要：研究电解液、电流密度和温度等阳极化条件对在 Al 5745 和 Al 1050A 基质上形成的氧化膜层摩擦因数和维氏硬度的影响。采用 DELTALAB HVS−1000 维氏硬度计和旋转销盘摩擦试验机测量样品的硬度和摩擦性能。结果表明：当草酸浓度为 10 g/L、电流密度为 3 A/dm^2 及温度为 5 °C 时，样品获得最高的维氏硬度(>HV 400)和最低的摩擦因数(<0.4)。采用辉光放电发生光谱法检测在 Al 5754 基质上形成的阳极氧化膜层上的氧化镁含量。氧化镁对膜层的力学性能产生一系列的负作用。最后，采用 SEM、EDS 和 AFM 测定摩擦试验前后阳极氧化膜的摩擦磨损性能。结果表明，磨损机理与材料的初始形貌、膜层的化学成分(C、S 和 Mg)、孔隙率和内应力等诸多因素有关。

关键词：铝合金；阳极化；摩擦因数；显微硬度；干滑动摩擦；表面表征

(Edited by Wei-ping CHEN)